Carbohydrate Polymers 87 (2012) 444–451

Contents lists available at ScienceDirect

Carbohydrate Polymers

journal homepage: www.elsevier.com/locate/carbpol

# Novel self-associative and multiphasic nanostructured soft carriers based on amphiphilic hyaluronic acid derivatives

Corinne Eenschooten[a,b,*], Andrea Vaccaro[c], Florence Delie[d], Fanny Guillaumie[a], Kristoffer Tømmeraas[a], Georgios M. Kontogeorgis[b], Khadija Schwach-Abdellaoui[a], Michal Borkovec[c], Robert Gurny[d]

[a] Novozymes Biopharma DK A/S, Krogshoejvej 36, DK-2880 Bagsværd, Denmark
[b] Technical University of Denmark, Department of Chemical and Biochemical Engineering, Centre for Energy Resources Engineering (CERE), Building 229, DK-2800 Lyngby, Denmark
[c] University of Geneva, Department of Inorganic, Analytical and Applied Chemistry, 30 quai Ernest-Ansermet, CH-1211 Geneva 4, Switzerland
[d] University of Geneva/Lausanne, School of Pharmaceutical Sciences, Department of Pharmaceutics and Biopharmaceutics, 30 quai Ernest-Ansermet, CH-1211 Geneva 4, Switzerland

ARTICLE INFO

*Article history:*
Received 12 January 2011
Received in revised form 24 May 2011
Accepted 3 August 2011
Available online 10 August 2011

*Keywords:*
Hyaluronic acid
Derivative
Self-assembly
Physicochemical properties
Polymeric nanogel
Drug delivery

ABSTRACT

The purpose of the present study was to investigate the physicochemical properties in aqueous media of amphiphilic hyaluronic acid (HA) derivatives obtained by reaction of HA's hydroxyl groups with octenyl succinic anhydride (OSA). The self-associative properties of the resulting octenyl succinic anhydride-modified hyaluronic acid (OSA-HA) derivatives were studied by fluorescence spectroscopy using Nile Red as fluorophore. The morphology, size and surface charge of the OSA-HA assemblies were determined by transmission electron microscopy, dynamic light scattering and by measuring their electrophoretic mobility, respectively. OSA-HA was shown to spontaneously self-associate in aqueous media into negatively charged spherical and multiphasic nanostructures with a hydrodynamic diameter between 170 and 230 nm and to solubilize hydrophobic compounds such as Nile Red. This was a good indication that OSA-HA could be used as building block for the formulation of soft nanocarriers towards the encapsulation and controlled delivery of hydrophobic active ingredients or drugs.



*Abbreviations:* $C_{10}$-HA, hyaluronic acid modified with alkyl chains containing 10 carbon atoms; $C_{12}$-HA, hyaluronic acid modified with alkyl chains containing 12 carbon atoms; $C_{18}$-HA, hyaluronic acid modified with alkyl chains containing 18 carbon atoms; CAC, critical aggregation concentration; C(domain), concentration of hydrophobic domains inside the polymeric micelles; $d_H$, average hydrodynamic diameter of the polymeric micelles; $d_i$, diameter of the polymeric micelle class *i*; DLS, dynamic light scattering; DS, degree of substitution; DVS, divinyl sulfone; $f_i$, probability density of the polymeric micelle class *i*; HA, hyaluronic acid; *l(between.domains)*, distance between vicinal hydrophobic domains in the polymeric micelles; *l(HAu)*, length of the HA unit; *l(OS)*, length of the octenyl succinate chain; MW, molecular weight; *MW(HAu)*, molecular weight of the HA unit; *MW(OSA)*, molecular weight of octenyl succinic anhydride; *n*, refractive index; $N_A$, Avogadro number; *N(domains)/micelle*, number of hydrophobic domains per polymeric micelle; *N(OSA-HAu)/domain*, number of modified units per hydrophobic domain; OS, octenyl succinate; OSA, octenyl succinic anhydride; OSA-HA, octenyl succinic anhydride-modified hyaluronic acid; OSA6-HA, octenyl succinic anhydride-modified hyaluronic acid with a degree of substitution equal to 6% per disaccharide unit; OSA18-HA, octenyl succinic anhydride-modified hyaluronic acid with a degree of substitution equal to 18% per disaccharide unit; OSA43-HA, octenyl succinic anhydride-modified hyaluronic acid with a degree of substitution equal to 43% per disaccharide unit; *P*, function defined in Eq. (2); PBS, phosphate buffered saline; *q*, scattering vector; RGD, Rayleigh–Gans–Debye; RHAMM, receptor for HA-mediated motility; *R(micelle)*, average radius of the most occurring polymeric micelle; Rt, room temperature; TEM, transmission electron microscopy; THF, tetrahydrofurane; *w(HAu)*, width of the HA unit; $\alpha$, swelling coefficient; $\lambda$, wavelength of light in vacuum; $\rho(HA)$, density of HA; $\rho(OSA\text{-}HA)$, density of OSA-HA; $\theta$, scattering angle.

* Corresponding author at: Novozymes Biopharma DK A/S, Krogshøjvej 36, DK-2880 Bagsværd, Denmark. Tel.: +45 4446 2599.
*E-mail address:* cnne@novozymes.com (C. Eenschooten).

0144-8617/$ – see front matter © 2011 Elsevier Ltd. All rights reserved.
doi:10.1016/j.carbpol.2011.08.004

## 1. Introduction

Hyaluronic acid (HA) is a natural linear polysaccharide consisting of D-glucuronic acid and *N*-acetyl-D-glucosamine linked through $\beta$-1,3 glycosidic bonds while consecutive disaccharide units are linked through $\beta$-1,4 bonds (Weissman & Meyer, 1954). HA is found in all mammalian tissues and is particularly abundant in the vitreous humor of the eye, the synovial fluid of the knee and the skin (Baier Leach & Schmidt, 2004). As biomacromolecule, HA possesses a large number of biological functions. It is for example known to mediate fundamental processes such as cell proliferation, differentiation and migration by binding with cells through specific interactions with hyaladherins such as the cellular receptor CD44 and the receptor for HA-mediated motility (RHAMM) (Baier Leach & Schmidt, 2004).

Due to its native unmatched biocompatibility and resorbability, physicochemical and biological properties as well as to the ease of its chemical functionalization, HA constitutes one of the most promising building blocks for applications in drug delivery (Gustafson, 1998). The use of native HA has already been widely studied towards ophthalmic, nasal, pulmonary and parenteral drug delivery (Liao, Jones, Forbes, Martin, & Brown, 2005). Indeed, when simply co-formulated together with a drug, HA has been shown to act as a mucoadhesive compound retaining the drug at its site of action and modifying the drug's in vivo absorption rate. Due to their relative poor complexity, these formulations can be classified as first generation HA-based drug delivery systems.

However, in cases of more challenging and demanding therapeutic situations, such as when drugs need to be protected and targeted to specific tissues, more advanced systems than co-formulations are required. In this regards, the interest of pharmacy in nanotechnology is explained by classical drug-associated issues such as poor drug solubility and instability in biological milieu (short drug half-life), poor drug bioavailability and unspecific targeting, which commonly result in the use of high drug dosages to achieve a therapeutic effect with the associated toxicity in patients and high health costs (Rawat, Singh, Saraf, & Saraf, 2006). As a consequence, the design of advanced drug delivery systems addressing these specific challenges has become more and more crucial and in this perspective, nanovehicles have often been put forward as a means to provide improved systems for the targeted and sustained/controlled delivery of drugs (Rawat et al., 2006). Second generation HA-based systems taking up a role as nanocarrier rather than simple excipient are therefore expected to be of tremendous significance for future pharmaceutical technologies.

However, the development of HA-based carriers is impeded by the high hydrophilicity and the poor biomechanical properties of the native molecule (Prestwich, Marecek, Marecek, Vercruysse, & Ziebell, 1998). The physicochemical properties of HA are indeed incompatible with the spontaneous and stable formation of segregated structures in aqueous media and the durable encapsulation of hydrophobic active ingredients or drugs. In addition, native HA displays a poor in vivo biological stability and residence time due to its relatively high turnover rate (Fraser, Laurent, & Laurent, 1997). A variety of chemical modifications have therefore been devised to provide HA with improved physicochemical properties and prolonged half life (Prestwich et al., 1998). In particular, the introduction of hydrophobic groups, for instance, alkyl chains onto the HA backbone has shown that the resulting HA derivatives exhibit significantly different physicochemical properties compared to the native polymer and that new associative systems can be created (Creuzet, Kadi, Rinaudo, & Auzley-Velty, 2006; Pelletier, Hubert, Lapicque, Payan, & Dellacherie, 2000). In a previous study, we developed a novel, simple and easily upscalable modification method for the preparation of amphiphilic HA derivatives based on the reaction between HA and octenyl succinic anhydride (OSA) in mild alkaline aqueous media (Tømmeraas & Eenschooten, 2007). The objective of this study was to investigate the physicochemical properties of a selection of OSA-HA derivatives. The self-associative properties of these derivatives were studied by fluorescence spectroscopy using Nile Red as fluorophore. The morphology, size and surface charge of the OSA-HA assemblies were determined by transmission electron microscopy, dynamic light scattering and by measuring their electrophoretic mobility, respectively. The results demonstrated that OSA-HA derivatives constitute attractive candidates for the formulation of soft nanocarriers towards the encapsulation and controlled and sustained delivery of hydrophobic active ingredients or drugs.

## 2. Materials and methods

### 2.1. Materials

The OSA-HA derivatives with a degree of substitution (DS) of 6, 18 and 43% per disaccharide unit (OSA6-HA, OSA18-HA and OSA43-HA) were prepared as described elsewhere (Eenschooten, Guillaumie, Kontogeorgis, Stenby, & Schwach-Abdellaoui, 2010). Briefly, HA (*Bacillus subtilis*-derived, Novozymes Biopharma DK A/S, Bagsværd, Denmark, with a weight average molecular weight of 21,000 Da) was first dissolved in milli-Q water at room temperature (Rt) for 6 h. $NaHCO_3$ was then added to the HA solution and mixed at Rt for 1 h. The pH of the resulting alkaline solution was measured and adjusted to 8.5 with NaOH (0.5 M). OSA was then added dropwise under vigorous stirring. The reaction medium was mixed at Rt for 16 h (overnight). The resulting crude product was collected and dialyzed against milli-Q water. The purified OSA-HA product was finally freeze-dried. Sodium chloride (NaCl), potassium chloride (KCl), disodium hydrogen phosphate ($Na_2HPO_4$), potassium dihydrogen phosphate ($KH_2PO_4$), tetrahydrofurane (THF), acetone, Nile Red and uranyl acetate were used as purchased without further purification. The water used for sample preparation or analysis was distilled and purified to a resistivity of 18.2 MΩ cm in a milli-Q apparatus. The physicochemical properties of the OSA-HA derivatives were investigated in a phosphate buffered saline (PBS, pH 7.4) which was prepared as followed: NaCl (8.0 g), KCl (0.2 g), $Na_2HPO_4$ (1.4 g) and $KH_2PO_4$ (0.2 g) were first dissolved in milli-Q water (1 L) for 1 h, at Rt. The pH of the resulting mixture was then measured and, if necessary, adjusted to 7.4 with HCl (0.2 M) or NaOH (0.2 M). The resulting buffer was finally filtered through glass microfiber filters (GF/F 1825 110, porosity 0.7 μm; Whatman, Maidstone, United Kingdom). The uranyl acetate solution used to stain the OSA-HA polymeric micelles for the transmission electron microscopy observations was a distilled water/saturated uranyl acetate mixture (60:40, v/v).

### 2.2. Methods

#### 2.2.1. Critical aggregation concentration of the OSA-HA derivatives

The critical aggregation concentration (CAC) of the OSA-HA derivatives was determined in PBS (pH 7.4) at 25 °C by fluorescence spectroscopy (FluoroMax; HORIBA Jobin Yvon Inc, Edison, New Jersey, United States) using Nile Red as fluorophore. OSA-HA was dissolved in PBS at the following concentrations: 0.001, 0.002, 0.004, 0.006, 0.008, 0.01, 0.02, 0.04, 0.06, 0.08, 0.1, 0.2, 0.4, 0.6, 0.8 and 1 g/L. The 0.2, 0.4, 0.6 and 0.8 g/L OSA-HA solutions were prepared from the 1-g/L OSA-HA solution by mixing 2, 4, 6 and 8 g of the latter into 8, 6, 4 and 2 g of PBS. Each of the remaining OSA-HA solutions was prepared from the 10-fold more concentrated OSA-HA solution by mixing 1 g of the solution into 9 g of PBS. Nile Red (3.184 mg) was dissolved in a THF/acetone mixture (50:50, v/v,

10 mL). A fraction of the resulting solution (0.01 mL) was added to each OSA-HA sample (10 mL) so that the final concentration of Nile Red in each sample was 1 μmol/L. The OSA-HA samples were stirred overnight, at room temperature and in the dark. Cuvettes were rinsed prior to use with 0.5 mL of the sample to be tested. Nile Red was excited at 543 nm and emission spectra were recorded from 580 to 700 nm. Three consecutive fluorescence spectra per sample were recorded. The emission spectra were fitted with a polynomial function (order 6) to determine the wavelength corresponding to the maximum intensity of the fluorescence emission. The averaged wavelengths were plotted as a function of the OSA-HA concentration for each derivative and the CAC was derived at the abscissa of the inflexion point of each plot.

#### 2.2.2. Morphology of the OSA-HA polymeric micelles

The morphology of the OSA-HA polymeric micelles was studied at room temperature by transmission electron microscopy (TEM, EM 410; Philips Electronic Instruments, Eindhoven, The Netherlands) using ionized carbon-coated copper grids and a uranyl acetate negative staining. OSA-HA (10 mg) was dissolved in PBS (10 mL) at room temperature, overnight. The carbon-coated copper grids were ionized for 20 s, under a pressure of 0.3 Torr and a voltage of 400 V and then deposited onto a 30-μL drop of the OSA-HA micellar solution for 30 s. Excess of the solution was drained from the grid which was then deposited onto a first 100-μL drop of uranyl acetate solution for a few seconds and immediately after onto a second 100-μL drop of uranyl acetate for 30 s. Excess of the solution was drained and the grid was dried prior to observation. Three grids per OSA-HA micellar solution were prepared and a minimum of four micrographs per grid were acquired at an accelerating voltage of 60 kV.

#### 2.2.3. Size distribution of the OSA-HA polymeric micelles

The size distribution of the OSA-HA polymeric micelles was first determined by extracting micelle diameters from TEM micrographs. The diameters of more than 600 micelles were individually and manually measured with the aid of the software ImageJ (United States National Institutes of Health, Bethesda, MA, United States). The size distribution obtained was fitted with the Schulz distribution (Schulz, 1939).

The hydrodynamic diameter of the OSA-HA polymeric micelles was then determined in PBS (pH 7.4), at room temperature, by dynamic light scattering (DLS) (ALV-CGS-8, equipped with a 532-nm solid-state laser as light source, ALV, Langen, Germany). OSA-HA (10 mg) was first dissolved in PBS (10 mL), at room temperature, overnight. The resulting solution was then filtered to remove dust particles. Four consecutive measurements of the diffusion coefficient per scattering angle were recorded from 20 to 120 °C. Measurements were performed at a polymer concentration of 1 mg/mL in order to allow an optimal signal to noise ratio. At this concentration and with the ionicity provided by the PBS buffer, the effect of particle-particle interactions can be neglected.

The hydrodynamic diameter of the OSA-HA polymeric micelles was also simulated, based on the size distribution obtained by TEM, by applying the Rayleigh–Gans–Debye (RGD) theory of dynamic light scattering (Berne & Pecora, 2000). Accordingly, the hydrodynamic diameter, $d_H$, is expressed as follows (Eq. (1)):

$$d_H(\theta) = \frac{\sum_i {d_i}^6 P((d_i/2)q) f_i}{\sum_i {d_i}^5 P((d_i/2)q) f_i} \quad (1)$$

where $\theta$, $d_i$, and $f_i$ represent the scattering angle (°), the diameter of the micelle class $i$ (nm) and the probability density of the micelle class $i$ ($nm^{-1}$), respectively.

$P((d_i/2)q)$ is the function defined in Eq. (2) and the expression for the modulus of the scattering vector $q$ ($nm^{-1}$) is given in Eq. (3) where $n$ and $\lambda$ represent the refractive index of the dispersion medium and the wavelength of light in vacuum (nm), respectively.

$$P\left(\frac{d_i}{2}q\right) = \frac{9}{((d_i/2)q)^6}\left(\sin\left(\frac{d_i}{2}q\right) - \left(\frac{d_i}{2}q\right)\cos\left(\frac{d_i}{2}q\right)\right)^2 \quad (2)$$

$$q = \frac{4\pi n}{\lambda}\sin\frac{\theta}{2} \quad (3)$$

The diameter values of the micelle classes in the size distribution obtained by TEM were adjusted so as to take into account micelle swelling. This was accomplished by introducing a swelling coefficient $\alpha$ which was defined as the ratio between the volume of water and the volume of OSA-HA making up fully hydrated micelles. As a result, diameter values of the micelle classes in the size distribution obtained by TEM were multiplied by the constant $\sqrt[3]{\alpha + 1}$.

#### 2.2.4. Zeta potential of the OSA-HA polymeric micelles

The zeta potential of the OSA-HA polymeric micelles (1 g/L) was determined in a diluted NaCl solution (0.001 mol/L), at 25 °C, by measuring their electrophoretic mobility (Zetasizer 3000 HS, Malvern, Worcestershire, United Kingdom). The pH of the solution was 3.8. Three consecutive measurements of the zeta potential were recorded per OSA-HA micellar solution.

## 3. Results and discussion

In a previous study, we developed a novel, simple and easily upscalable modification method for the preparation of amphiphilic HA derivatives based on the reaction between HA and octenyl succinic anhydride in mild alkaline aqueous media (Tømmeraas & Eenschooten, 2007) (Fig. 1). In the present study, we investigated the solution and physicochemical properties of a selection of OSA-HA derivatives with a degree of substitution of 6, 18 and 43% per disaccharide unit.

### 3.1. Critical aggregation concentration of the OSA-HA derivatives

The introduction of octenyl succinate (OS) groups onto HA is expected to alter the solution properties of the native HA and in particular the intra- and intermolecular interactions between HA chains. The CAC of a selection of OSA-HA derivatives was determined in PBS (pH 7.4) at 25 °C by fluorescence spectroscopy using Nile Red as fluorophore.

The fluorescence response of Nile Red and more specifically its maximum fluorescence emission wavelength is dependent on the polarity of its surrounding environment. Such wavelength is lower in non-polar environments than in polar medium (Dutt & Doriswami, 1992). Due to this intrinsic property, Nile Red can be used to determine the CAC of associative amphiphilic polymers in aqueous media. Indeed, this physical transition typically involves the formation of segregated non-polar colloidal domains where Nile Red can be readily incorporated.

For our purpose, Nile Red was added to a series of OSA-HA/PBS solutions with concentrations ranging from 0.001 to 1 g/L. The PBS was used to buffer both ionic strength and acidity variations among the different OSA-HA samples. The maximum fluorescence emission wavelength of Nile Red was followed as a function of the OSA-HA concentration and was plotted for OSA-HA derivatives with a DS of 6, 18 and 43% (Fig. 2). The results show that independently on the DS of the derivative, the maximum fluorescence emission wavelength of Nile Red rapidly decreased from about 650 to 610 nm when the OSA-HA concentration increased. This abrupt wavelength change indicates that the immediate environment of the fluorescent dye changed from polar to less polar owing to the interactions between Nile Red and the OS pendant groups during

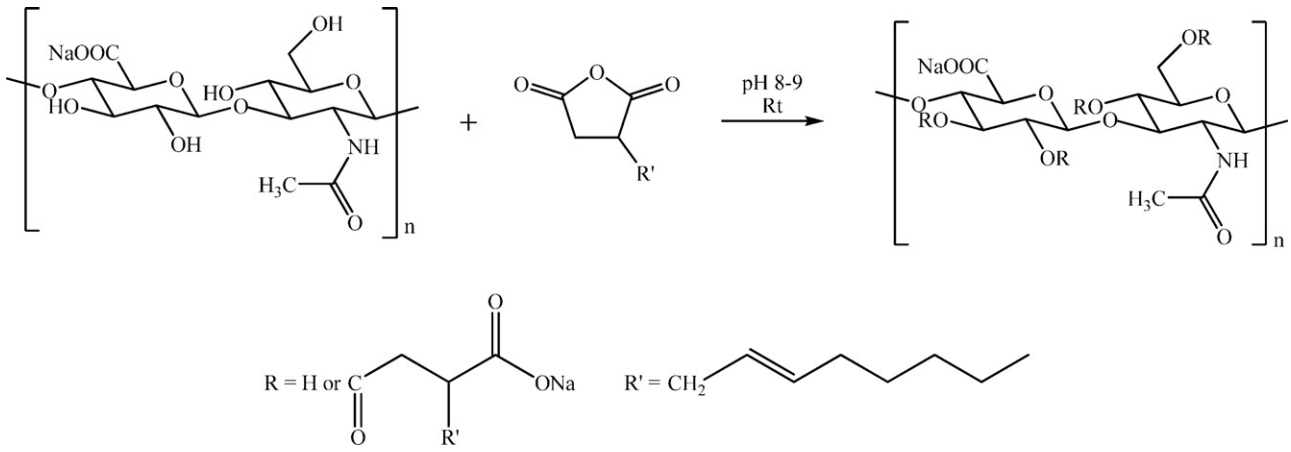


**Fig. 1.** Modification of HA with OSA. Reactions were conducted in $NaHCO_3$-buffered solutions (0.2–1.0 M), at pH 8–9, at room temperature and for between 6 and 24 h.

the formation of the OSA-HA assemblies. Furthermore, the concentration at which this transition was observed was dependent on the DS of the OSA-HA derivative. Indeed, when plotted as a function of the derivatives' DS, the CAC linearly decreased with increasing the degree of modification of the polymer ($CAC = -0.0023DS + 0.1111$; $R^2 = 0.9918$): the higher the DS of the derivative, the stronger the attraction between the OS pendant groups. A higher hydrophobicity of the derivatives results in the formation of OSA-HA assemblies at a lower concentration.

Interestingly, the polymer concentration values corresponding to the formation of hydrophobic domains found in the present work (0.015–0.1 g/L) were of the same order of magnitude as those previously reported for some alkylated HA derivatives. For instance, Pelletier et al. (2000) have shown using fluorescence spectroscopy and pyrene as probe that 480,000-Da HA modified with alkyl chains containing 12 carbon atoms ($C_{12}$-HA, DS = 5%) and 18 carbon atoms ($C_{18}$-HA, DS = 2%) self-associated and formed hydrophobic domains in which pyrene was solubilized at polymer concentrations of 0.05 g/L ($C_{12}$-HA) and 0.01 g/L ($C_{18}$-HA). Likewise, Creuzet et al. (2006) have shown using a similar experimental procedure that 300,000-Da HA modified with alkyl chains containing 10 carbon atoms ($C_{10}$-HA, DS = 5%) and 12 carbon atoms ($C_{12}$-HA, DS = 4%) rearranged into polymeric aggregates at polymer concentrations between 0.01 and 0.1 g/L. Although a direct comparison between these results and those of the present study is made difficult by the differences in initial HA molecular weight (MW), modification chemistry, nature of the hydrophobic pendant groups and DS, the order of magnitude of the OSA-HA concentrations at which self-association occurred indicates a relatively good consistency with the literature.

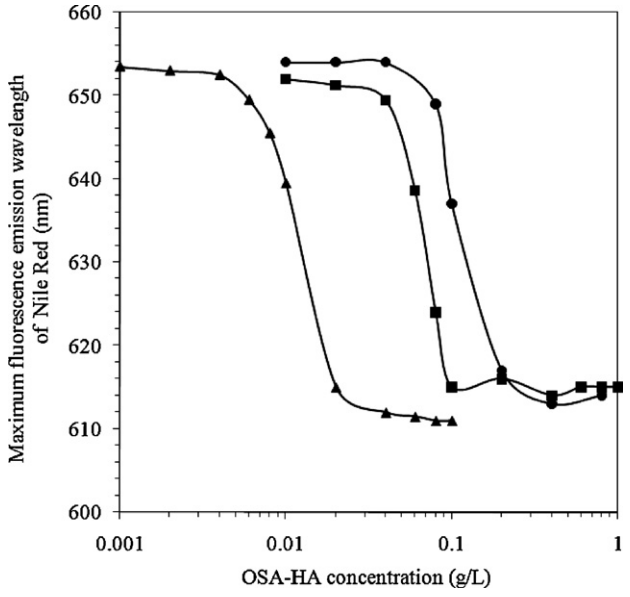


**Fig. 2.** Maximum fluorescence emission wavelength of Nile Red as a function of the OSA-HA concentration in PBS (pH 7.4) at 25 °C for a series of OSA-HA derivatives with different degrees of substitution. ●, OSA6-HA; ■, OSA18-HA; and ▲, OSA43-HA.

In summary, OSA-HA with a DS between 6 and 43% was demonstrated to behave like an amphiphilic polymer which can self-associate in aqueous media into polymeric micelles and solubilize a hydrophobic compound such as Nile Red above a CAC which depends on the DS of the derivative. Micellization of OSA-HA is therefore a controllable property through the DS of the derivative and can be predicted for modified polymers with a DS between 6 and 43%.

Due to its highest hydrophobic character, OSA43-HA was chosen as a model compound for the detailed study of the morphology, size distribution, surface charge and molecular structure of the OSA-HA polymeric micelles.

### 3.2. Morphology of the OSA43-HA polymeric micelles

The morphology of the OSA43-HA polymeric micelles was studied at Rt by transmission electron microscopy using a uranyl acetate negative staining. A selection of micrographs acquired at two different scales is presented in Fig. 3. The micrograph on the left of the figure shows that the OSA43-HA polymeric micelles were relatively polydisperse spherical objects with a dry diameter ranging between 10 and 120 nm. The difference in size between the micelles was most likely due to a discrepancy in the number of OSA43-HA molecules involved in each micelle. This could be imputable to a possible heterogeneous DS among the OSA43-HA molecules or to a potential irregular repartition of OS groups along the HA chains.

The set of four micrographs on the right of Fig. 3 shows that the micelle structure is non-uniform which suggests that the micelles are composed of distinct colloidal domains which could consist of segregated non-polar poaches embedded into a polar polymeric matrix (see also Section 3.5 and Fig. 7).

### 3.3. Size distribution of the OSA43-HA polymeric micelles

In order to determine the size distribution of the OSA43-HA polymeric micelles more precisely, a statistical analysis of the micelles' diameter on the TEM micrographs was conducted in parallel to DLS measurements.

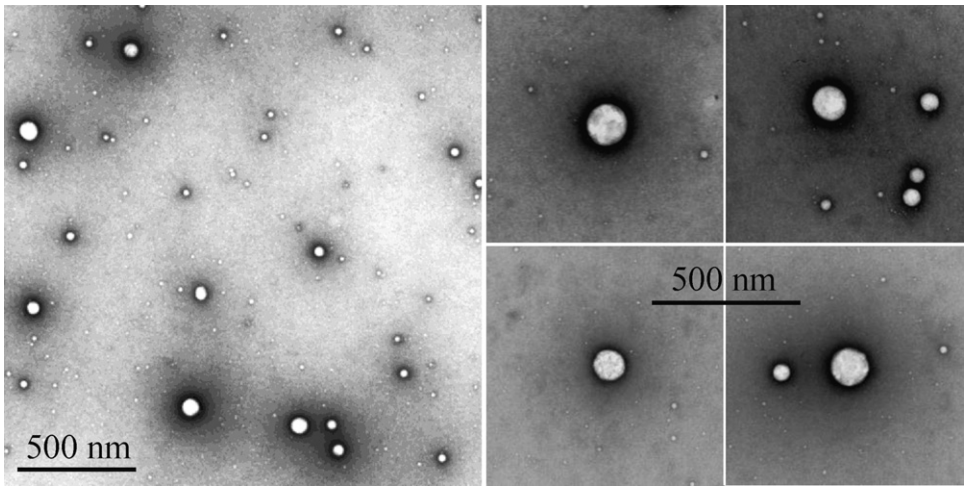


**Fig. 3.** Selected transmission electron micrographs of the OSA43-HA polymeric micelles. Prior to deposition onto the ionized carbon-coated copper grids, the OSA43-HA samples were prepared in PBS (pH 7.4) at a polymer concentration of 1 g/L.

Microscopy and DLS can both give information about the size of colloids, although in a different manner, since they are based on different physical principles. When studied by microscopy, the size of colloids is obtained directly. However, sample preparation and observation conditions can alter their properties and therefore their size. In this study, the OSA43-HA polymeric micelles were observed in a dry state under vacuum, which most likely caused them to shrink. For this reason, their size was subsequently adjusted by means of a swelling coefficient to permit comparison with the DLS data. When studied by DLS, the size of colloids is obtained indirectly since it is derived from colloidal diffusion in solution by means of the Stokes–Einstein equation which implies a number of assumptions. However, no sample preparation other than suspending the colloids in solution is required and the colloids are analyzed *in situ*. Given these principles, microscopy and DLS were used in combination to obtain statistical and reliable information about the size of the OSA43-HA polymeric micelles.

The number-weighed size distribution of the OSA43-HA polymeric micelles obtained by statistically extracting micelle diameters from TEM micrographs with the software ImageJ is presented in Fig. 4. The results confirmed that the OSA43-HA micelles had a dry diameter between 10 and 120 nm and that there were only a few micelles with a size above 60 nm. Most of micelles had a diameter between 10 and 20 nm. The arithmetic average micelle diameter was 26 nm (standard deviation = 15 nm) which evidenced a non-negligible size polydispersity.

The cumulative size distribution of the OSA43-HA polymeric micelles (Fig. 5) revealed that 80% of the micelles had a diameter below 25 nm. When applying the Schulz model to these experimental data, the best fits were obtained with the following parameters: $\sigma = 4.82$ and $\mu = 16.02$. The fit was excellent up to a cumulative frequency of 0.80 from which it deviated from the experimental data between 0.80 and 0.95. This was due to the presence of the larger micelle population, which the models could not account for.

The hydrodynamic diameter of the OSA43-HA polymeric micelles was determined in PBS (pH 7.4) by DLS and was also simulated from the statistical microscopy data. Fig. 6 presents the variation of the hydrodynamic diameter as a function of the scattering angle as measured by DLS and as simulated from the micelle size distribution presented above for two different values of the swelling coefficient $\alpha$ ($\alpha = 0$ for dehydrated micelles and $\alpha = 12$ g of water/g of polymer for hydrated micelles). The results show that the values of hydrodynamic diameter measured by DLS were about twice as large as those simulated from the crude microscopy data, i.e. when $\alpha = 0$. Indeed, the OSA43-HA polymeric micelles were hydrated during the DLS analysis, whereas they had lost their water content before the TEM analysis. Taking into account micelle hydration in the simulation ($\alpha = 12$ g of water/g of polymer), a better fit was obtained between the hydrodynamic diameter values obtained by DLS and those obtained by TEM over most of the scattering angles, especially between 30° and 100°. This indicated that the micelles in solution contained a volume of water of up to 12 times the volume of OSA43-HA making up fully hydrated micelles. The fairly large deviation of the hydrodynamic diameter measured by DLS from that simulated by microscopy (with $\alpha = 12$) at low scattering angles indicated that a few structures with dimensions superior to the detection range of the DLS instrument were present in solution. These few structures could be micelle aggregates although micelle aggregation could not clearly be identified on the TEM micrographs. Interestingly, the swelling coefficient found in this study was of the same order of magnitude as previously reported values of the swelling ratio in chemically crosslinked HA hydro-

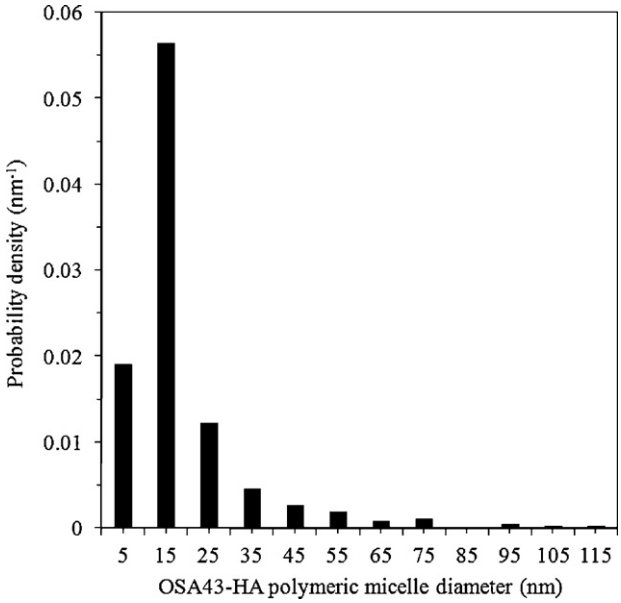


**Fig. 4.** Number-weighed size distribution of the OSA43-HA polymeric micelles based on micelle diameter extraction from TEM micrographs.

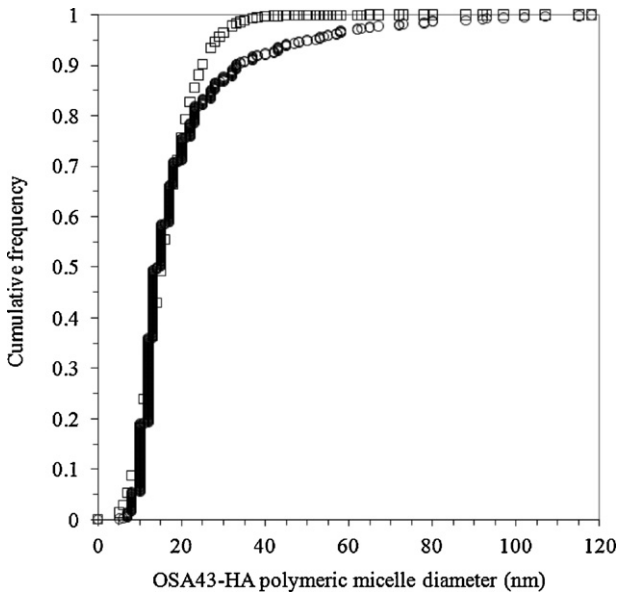


**Fig. 5.** Number-weighed cumulative size distribution of the OSA43-HA polymeric micelles based on micelle diameter extraction from TEM micrographs. ○, Microscopy data; □, Schulz fit. $f_{\text{Schulz}}(x) = \left[\frac{\sigma+1}{\mu}\right]^{\sigma+1} \frac{x^{\sigma}}{\Gamma(\sigma+1)} \exp\left[-\frac{\sigma+1}{\mu}x\right]$, $\Gamma(a) = \int_0^{\infty} t^{a-1} \exp(-t)dt$.

gels. Srinivas and Ramamurthi (2007) have indeed reported that the swelling ratio of HA hydrogels obtained by crosslinking HA chains with divinyl sulfone (DVS) (HA/DVS weight ratio = 3) could reach values up to 7. In that study, the swelling ratio was defined as the ratio of the difference between the weight of the swollen and the dried gel to the weight of the dried gel obtained by freeze-drying. Since TEM micrographs are acquired under vacuum, the degree of dehydration of these hydrogels is comparable to that of the OSA43-HA polymeric micelles observed by TEM. It could be demonstrated that the definition of the swelling ratio by Srinivas and Ramamurthi is equivalent to that of the present study if the density of OSA43-HA is close to 1.0. Therefore the value of swelling

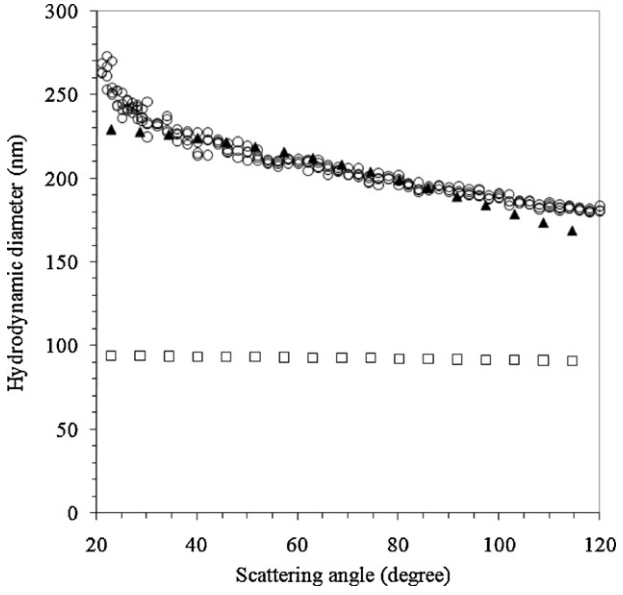


**Fig. 6.** Experimental and simulated hydrodynamic diameter of the OSA43-HA polymeric micelles as a function of the scattering angle. ○, Dynamic light scattering data; □, Simulated microscopy data with $\alpha = 0$; and ▲, Simulated microscopy data with $\alpha = 12$ g of water/g of polymer.

coefficient found in this study (12) can be directly compared to that found by Srinivas and Ramamurthi (7). Similarly, Smeds et al. (2001) observed that HA hydrogels obtained by photo-crosslinking methacrylated HA could swell up to 11 times their dry weight when the dried gels were obtained by freeze drying. This swelling ability was dependent on the degree of crosslinking. The gels with the highest degree of crosslinking had the least ability to swell due to their tighter polymeric networks. In that study, the swelling coefficient was defined as the ratio of the weight of the swollen gel to that of the dried gel. It could be shown that the relationship between this swelling ratio A and the swelling ratio $\alpha$ defined in the present study is $\alpha = A - 1$ if the density of OSA43-HA is close to 1.0. In other words, the value of the swelling coefficient found in the present study (12) is to be compared with an adjusted value of 10. This comparison with existing literature on HA hydrogels shows that the OSA43-HA polymeric micelles exhibit comparable swelling properties as chemically crosslinking HA. However, unlike HA hydrogels which are stabilized by chemical crosslinking, OSA43-HA polymeric micelles owe their structure to hydrophobic interactions. This suggests regarding OSA43-HA polymeric micelles as physically crosslinked nanogels. In summary, the data provided by the microscopy and DLS analysis show that the OSA43-HA polymeric micelles are highly hydrated structures in solution with a mean hydrodynamic diameter falling between 170 and 230 nm. The value of swelling coefficient used to correlate the microscopy and DLS data is comparable to that of chemically crosslinked HA hydrogels which suggests that the OSA43-HA polymeric micelles are physically crosslinked nanogels stabilized by the hydrophobic interactions between the OS pendant groups.

### 3.4. Zeta potential of the OSA43-HA polymeric micelles

The zeta potential of the OSA43-HA polymeric micelles was determined in a diluted NaCl solution (0.001 mol/L), at 25 °C, by measuring their electrophoretic mobility. The surface of the OSA43-HA polymeric micelles was shown to be negatively charged with a zeta potential of approximately −28 mV under the applied conditions (pH ~3.0–4.0). This negative charge was due to the presence of carboxylate groups on OSA43-HA arising from both the native HA backbone and the hemiesters generated during the reaction between HA and OSA. Comparison of this charge with that of the unmodified polymer was impossible since the signal for isolated polymers was much lower than for the micelles. The magnitude of the micelles' negative charge gives an indication that these structures are fairly stable in solution.

### 3.5. Molecular structure of the OSA43-HA polymeric micelles

Chen et al. (2005) have described the structure of polymeric micelles based on hydrophobically modified HA with 2,300 Da poly(caprolactone) chains as a spherical HA hydrophilic corona surrounding a poly(caprolactone) hydrophobic core. Given the relatively short length of the OS pendant groups, the aggregation of OSA43-HA is unlikely to occur in this fashion.

Assuming that, due to the flexibility of HA, modified disaccharide units of OSA43-HA can behave like monomeric surfactant moieties capable of self-associating into conventional spherical monomeric micellar domains, OSA43-HA polymeric micelles are believed to consist of a dispersion of hydrophobic domains formed by the modified HA units in a hydrophilic matrix structured by the remaining unmodified HA units (Fig. 7). In this multiphasic model, the OS groups involved in the hydrophobic domains can originate from the same or different OSA43-HA molecules and the micelle structure is believed to be stabilized by a combination of hydrophobic interactions between the OS groups and the fundamental structures of non-modified HA in aqueous media, in particular the

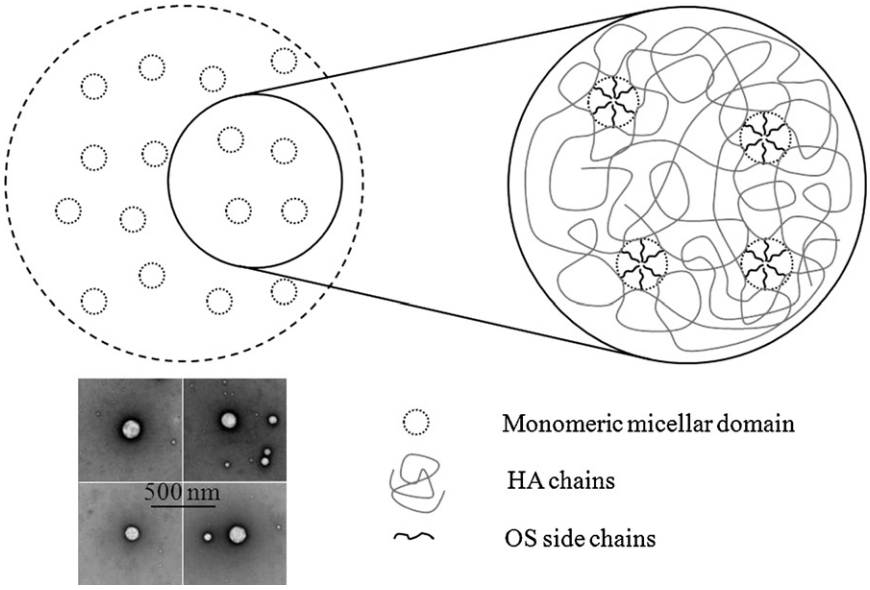


**Fig. 7.** Tentative representation of the structure of the OSA43-HA polymeric micelles.

intra- and intermolecular hydrogen bonding between HA chains (Scott, 1998). The number of substituted HA units per hydrophobic domains, of hydrophobic domains per micelle and the average distance between vicinal hydrophobic domains were calculated for the most occurring micelle, i.e. a micelle with a radius of approximately 8 nm in the dehydrated state (see Fig. 4) or 19 nm in the hydrated state. The dimensions of the modified disaccharide unit used in the calculations were the following: the length and width of the disaccharide unit were approximated to 1 and 0.5 nm, respectively (Ionov, El-Abed, Goldmann, & Peretti, 2004). The length of the OS chains was approximated to 1 nm as it consists of about 10 carbon-to-carbon bonds. It should be noted that the influence of the geometric isomerism of the OS chains (*cis*/*trans*) on the packing of the hydrophobic domains was disregarded as the distribution of the *cis* and *trans* OS moieties on HA was unknown. In the following calculations, the densities of HA and OSA43-HA were considered to be close to 1.0 g/cm$^3$.

The number of modified disaccharide units per hydrophobic domain was calculated by dividing the volume of one hydrophobic domain by the volume of one modified unit. The volume of one modified unit can further be decomposed as the sum of the volume of one HA unit and the volume of the cone deployed by one OS chain. Substitution with more elementary physical quantities leads to Eq. (4) where *N*(OSA-HA*u*)*/domain*, *w(HAu)*, *l(OS)*, *MW(HAu)*, *ρ(HA)*, $N_A$ and *l(HAu)* represent the number of modified units per hydrophobic domain, the width of the HA unit, the length of the OS chain, the molecular weight of the HA unit, the density of HA, the Avogadro number and the length of the HA unit, respectively.

$$N(\text{OSA-HAu})/domain = \frac{(4/3)\pi(w(HAu)+l(OS))^3}{(MW(HAu)/\rho(HA)N_A)+(1/3)\pi(l(HAu)/2)^2 l(OS)} \quad (4)$$

The number of hydrophobic domains per micelle was calculated by dividing the number of modified units per micelle by the number of modified units per hydrophobic domain. The number of modified units per micelle corresponds to the number of OSA-HA molecules per micelle multiplied by the number of modified units per OSA-HA molecule. This number is related to the DS of OSA-HA. The number of OSA-HA molecules per micelle can be calculated by dividing the volume of one micelle by the volume of one OSA-HA molecule. Subsequent substitutions and rearrangements leads to Eq. (5) where *N(domains)/micelle*, *R(micelle)*, *ρ*(OSA-HA*)*, $N_A$, *MW(HAu)*, *DS*, *MW(OSA)* and *N(OSA-HAu)/domain* stand for the number of hydrophobic domains per micelle, the average radius of the most occurring micelle, the density of OSA-HA, the Avogadro number, the molecular weight of the HA unit, the degree of substitution of OSA-HA (here 43%), the molecular weight of OSA and the number of modified unit per hydrophobic domain, respectively.

$$N(domains)/micelle = \frac{((4/3)\pi R(micelle)^3 \rho(OSA-HA)N_A)/((MW(HAu)/DS)+MW(OSA))}{N(OSA\text{-}HAu)/domain} \quad (5)$$

Finally, the distance between vicinal hydrophobic domains was calculated by applying the relation shown in Eq. (6) where *l(between.domains)* and *C(domain)* correspond to the distance between vicinal hydrophobic domains and concentration of hydrophobic domains inside the micelle, respectively.

$$l(between.domains) = \sqrt[3]{\frac{1}{C(domains)}} \quad (6)$$

The concentration of hydrophobic domains inside the micelle can be expressed as the ratio of the number of hydrophobic domains per micelle to the volume of the hydrated micelle as shown in Eq. (7) where *l(between.domains)*, *α*, *R(micelle)* and *N(domains)/micelle* represent the distance between vicinal hydrophobic domains, the swelling coefficient defined earlier, the radius of the most occurring micelle and the number of hydrophobic domains per micelle, respectively.

$$l(between.domains) = \sqrt[3]{\frac{(4/3)\pi(\sqrt[3]{\alpha+1}R(micelle))^3}{N(domains)/micelle}} \quad (7)$$

According to our calculations, the most occurring OSA43-HA micelle would consist of about 72 hydrophobic domains separated by a distance of 6–9 nm, with a diameter of 3 nm and each containing 16 modified units (Table 1). Although approximate, this model is believed to provide a rough but realistic picture of the internal structure of the micelles.

**Table 1**
Characteristics of the most occurring OSA43-HA polymeric micelle according to the molecular model developed.

| Characteristic dimension | Symbol | Value |
|---|---|---|
| Dehydrated radius | $R(micelle)$ | 8 nm |
| Hydrated radius | $\sqrt[3]{\alpha+1}R(micelle)$ | 19 nm |
| No. of hydrophobic domain per micelle | $N(domains)/micelle$ | 72 |
| No. of modified disaccharide units per hydrophobic domain | $N(OSA\text{-}HAu)/domain$ | 16 |
| Distance between vicinal hydrophobic domains | $l(between.domains)$ | 6–9 nm |

## 4. Conclusion

Partially water-soluble amphiphilic octenyl succinic anhydride-modified hyaluronic acid derivatives were prepared and their solution and physicochemical properties were investigated in aqueous media. These included the determination of the critical aggregation concentration of the HA derivative as well as the study of fundamental properties of the resulting polymeric micelles such as morphology, size distribution and surface charge. OSA-HA was shown to spontaneously self-associate in aqueous media into polymeric assemblies capable of solubilizing Nile Red into the hydrophobic domains formed by the octenyl succinic groups. This transition from random coil to particulate system occurred above a CAC which was dependent on the degree of substitution of the derivatives. The CAC of OSA-HA was indeed a linear decreasing function of the derivatives' DS between 6 and 43% per disaccharide unit and it can be predicted for OSA-HA derivatives with a DS in this range. The OSA-HA polymeric micelles were negatively charged spherical objects characterized by a high degree of hydration (typically 12 g of water per g of polymer) and a mean hydrodynamic diameter between 170 and 230 nm. The high water content derived from this study was similar to values reported for chemically crosslinked HA hydrogels which suggests regarding the OSA-HA polymeric micelles as physically crosslinked nanogels. The internal structure of the OSA-HA nanogels is believed to consist of a dispersion of hydrophobic monomeric micellar domains formed by the OS groups embedded in a hydrophilic polymeric matrix composed of the unmodified HA segments. The stabilization mechanism of these structures was attributed to a combination of hydrophobic interactions between the OS groups and the fundamental structures of non-modified HA in aqueous media, in particular intra- and intermolecular hydrogen bonding between HA chains.

Whereas most of the currently available methods for the preparation of HA nanoparticles rely on random collisions in the medium to create structures, a novel molecular technique was here developed which relies on the controlled self-assembly of amphiphilic HA leading to multiphasic nanoarchitectured HA-based assemblies. We therefore believe that the OSA-HA nanogels described here will constitute a valuable first step towards formulating HA-based nanoparticles with more complex configurations than single ingredient or core-shell structures. In particular, the presence of multiple hydrophobic substructures inside the nanogels could be used to encapsulate hydrophobic active ingredients or drugs and sustain their release in biological environments. Moreover, it should be emphasized that the methods underlying the nanogels are simple, aqueous and easily upscalable and that the nanogels are expected to retain the biocompatibility and resorbability of native HA. This makes them potentially valuable for industrial pharmaceutical applications. Finally, the modification method increases the distribution of negative charges along the modified polymer at neutral pH which constitutes an advantage for the electrostatic stabilization of the nanogels.

The formulation of OSA-HA nanoparticles insensitive to dilution and the study of the release of model hydrophobic substances encapsulated in the particles *in vitro* and in vivo will be the subject of future investigations.

## Conflicts of interest

The authors report no conflicts of interest. The authors alone are responsible for the content and writing of the paper.

## Acknowledgments

The Danish Ministry of Science, Technology and Innovation (Grant No. 07-001687) and Novozymes Biopharma DK A/S are gratefully acknowledged for their generous funding.

## References

Baier Leach, J., & Schmidt, C. E. (2004). Hyaluronan. In G. E. Wnek, & G. L. Bowlin (Eds.), *Encyclopaedia of biomaterials and biomedical engineering* (pp. 779–789). Marcel Dekker: New York.

Berne, B. J., & Pecora, R. (2000). *Dynamic light scattering*. Mineola: Dover Publications.

Chen, J. H., Tsai, B. H., Chang, H. T., Chen, M. L., Chen, Y. H., Jan, S. H., & Liu, M. J. (2005). Biodegradable hyaluronic acid derivative and biodegradable polymeric micelle composition. *United States Patent and Trademark Office*, Pat. No. US 2005/0123505 A1.

Creuzet, C., Kadi, S., Rinaudo, M., & Auzley-Velty, R. (2006). New associative systems based on alkylated hyaluronic acid. Synthesis and aqueous solution properties. *Polymer*, *47*, 2706–2713.

Dutt, G. B., & Doriswami, S. (1992). Picosecond reorientational dynamics of polar dye probes in binary aqueous mixtures. *The Journal of Chemical Physics*, *96*, 2475–2491.

Eenschooten, C., Guillaumie, F., Kontogeorgis, G. M., Stenby, E. H., & Schwach-Abdellaoui, K. (2010). Preparation and structural characterisation of novel and versatile amphiphilic octenyl succinic anhydride-modified hyaluronic acid derivatives. *Carbohydrate Polymers*, *79*, 597–605.

Fraser, J. R., Laurent, T. C., & Laurent, U. B. (1997). Hyaluronan: Its nature, distribution, functions and turnover. *Journal of Internal Medicine*, *242*, 27–33.

Gustafson, S. (1998). Hyaluronan in drug delivery. In T. C. Laurent (Ed.), *The chemistry, biology and medical applications of hyaluronan and its derivatives* (pp. 291–304). Portland Press: London.

Ionov, R., El-Abed, A., Goldmann, M., & Peretti, P. (2004). Interactions of lipid monolayers with the natural biopolymer hyaluronic acid. *Biochimica et Biophysica Acta*, *1667*, 200–207.

Liao, Y. H., Jones, S. A., Forbes, B., Martin, G. P., & Brown, M. B. (2005). Hyaluronan: Pharmaceutical characterization and drug delivery. *Drug Delivery*, *12*, 327–342.

Pelletier, S., Hubert, P., Lapicque, F., Payan, E., & Dellacherie, E. (2000). Amphiphilic derivatives of sodium alginate and hyaluronate: Synthesis and physico-chemical properties of aqueous dilute solutions. *Carbohydrate Polymers*, *43*, 343–349.

Prestwich, G. P., Marecek, D. M., Marecek, J. F., Vercruysse, K. P., & Ziebell, M. R. (1998). Chemical modification of hyaluronic acid for drug delivery, biomaterials and biochemical probes. In T. C. Laurent (Ed.), *The chemistry, biology and medical applications of hyaluronan and its derivatives* (pp. 43–65). London: Portland Press.

Rawat, M., Singh, D., Saraf, S., & Saraf, S. (2006). Nanocarriers: Promising vehicle for bioactive drugs. *Biological & Pharmaceutical Bulletin*, *29*, 1790–1798.

Schulz, G. V. (1939). The kinetics of chain polymerisation V. The influence of various types of reactions on the poly-molecularity. *Zeitschrift für physikalische Chemie Abteilung B*, *43*, 25–46.

Scott, J. E. (1998). Secondary and tertiary structures of hyaluronan in aqueous solution. Some biological consequences. http://www.glycoforum.gr.jp/science/hyaluronan/hyaluronanE.html.

Smeds, K. A., Pfister-Serres, A., Miki, D., Dastgheib, M., Inoue, M., Hatchell, D. L., et al. (2001). Photocrosslinkable polysaccharides for *in situ* hydrogel formation. *Journal of Biomedical Materials Research*, *55*, 254–255.

Srinivas, A., & Ramamurthi, A. (2007). Effects of gamma-irradiation on physical and biologic properties of cross-linked hyaluronan tissue engineering scaffolds. *Tissue Engineering*, *13*, 447–459.

Tømmeraas, K., & Eenschooten, C. (2007). Aryl/alkyl succinic anhydride hyaluronan derivatives. *World Intellectual Property Organization*, Pat. No. WO 2007/033677 A1.

Weissman, B., & Meyer, K. (1954). The structure of hyalobiuronic acid and of hyaluronic acid from umbilical cord. *Journal of the American Chemical Society*, *76*, 1753–1757.